Electronic Supplementary Material (ESI) for CrystEngComm.

Supporting Information

High tuneable proton-conducting coordination polymers derived from sulfonate-based ligand

Mei-Jie Wei, Jia-Qi Fu, Yi-Di Wang, Yi Zhang, Hong-Ying Zang*, Kui-Zhan Shao, Yang-Guang Li*, Zhong-Min Su*

Key Lab of Polyoxometalate Science of Ministry of Education, Institute of Functional Material Chemistry Faculty of Chemistry, Key Laboratory of Nanobiosensing and Nanobioanalysis at Universities of Jilin Province, Faculty of Chemistry, Northeast Normal University, Changchun 130024, Jilin (P. R. China).

Experimental Section

Materials and Characterization. The commercially available chemical reagents employed in the experiment were used without further purification. The ligand was synthesized with similar methods as reported in the literature.[1] HCl steaming-assisted conversion approach was developed based on previous synthetic method, in which we used 1 M HCl instead of H_2O.[2] Thermogravimetric analysis (TGA) data was performed on a Perkin-Elmer TGA analyzer at a heating rate of 10 °C/min under a N_2 atmosphere. Differential scanning calorimeter (DSC) data were carried out with a NETZSCH STA 449F3 analyzer in a heating rate of 10 °C/min under a N_2 atmosphere. Elemental analyses were determined from a Perkin-Elmer 2400 elemental analyzer. FTIR spectra were measured at a Nicolet Magna 560 IR spectrometer. Powder X-ray diffraction (PXRD) patterns were conducted on a Siemens D 5005 diffractometer. Quantachrome Autosorb-iQ was used to measure the N_2 gas adsorption isotherm. Water vapor adsorption measurement were performed on Hidenisochema IGA 100B instrument at 298 K.

Synthesis of $Cu_2H_2(Hspip)_2Cl_4 \cdot H_2O$. A mixture of $Cu(CH_3COO)_2$ (8.0 mg, 0.0440 mmol) and H_2spip (17 mg, 0.0452 mmol) were put into a home-made glass tube in a sealed Teflon steel filled with 5 mL of 1 M HCl. The mixture was heated at 170 °C for 72 h. In the end, the green crystals were collected, yield: ~60% based on Cu. Elemental analysis calcd. for $C_{38}H_{26}N_8O_7Cu_2S_2Cl_4$ (%): C, 43.90; H, 2.52; N, 10.78; found: C, 43.29; H, 2.41; N, 10.63. IR (KBr): ν= 3444 (m), 3070 (m), 1647 (m), 1620 (m), 1591 (m), 1562 (s), 1518 (m), 1446 (s), 1431 (w), 1404 (s), 1278 (s), 1251 (w), 1230 (m), 1196 (m), 1174 (s), 1126 (m), 1080 (m), 1045 (w), 1022 (m), 976 (m), 947 (m), 879 (m), 819 (m), 773 (m), 748 (m), 731 (m), 711 (m), 659 (m), 644 (m), 611 (s), 574 (m), 551 (m), 515 (m).

Synthesis of $Cu(H_2spip)Cl_2 \cdot H_2O$. A mixture of copper tartrate trihydrate (12.0 mg, 0.0452 mmol), $H_2C_2O_4 \cdot 2H_2O$ (22 mg, 0.1745 mmol) and H_2spip (17 mg, 0.0452 mmol) were put into a home-made glass tube in a sealed Teflon steel filled with 5 mL of 1 M HCl. The hybrid was heated at 170 °C for 72 h. At last, the green crystals were synthesized, yield: ~51% based on Cu. Elemental analysis calcd. for $C_{19}H_{14}N_4O_4CuSCl_2$ (%): C, 43.15; H, 2.67; N, 10.59; found: C, 42.81; H, 2.47; N, 10.76. IR

(KBr): *v*= 3446 (m), 3074 (m), 1649 (m), 1620 (m), 1587 (m), 1562 (s), 1519 (m), 1446 (s), 1404 (s), 1334 (m), 1263 (s), 1232 (m), 1194 (m), 1165 (m), 1081 (m), 1047 (w), 1016 (m), 976 (m), 945 (m), 879 (m), 816 (m), 785 (m), 748 (m), 727 (m), 711 (w), 654 (m), 613 (s), 573 (m), 557 (m), 515 (w).

Synthesis of CuH(Hspip)(HPO$_4$)·H$_2$O. A mixture of Cu(CH$_3$COO)$_2$ (4.0 mg, 0.0220 mmol) and H$_2$spip (10.0 mg, 0.0266 mmol) was dissolved in distilled water (10 mL). Next, the pH was regulated to 1.2 with addition of 2.5 mol/L H_3PO_4. The mixture was heated inside a sealed Teflon steel at 170 °C for 72 h. Finally, the green crystals were gathered, yield: ~45% based on Cu). Elemental analysis calcd. for $C_{19}H_{15}N_4O_8CuSP$ (%): C, 41.20; H, 2.73; N, 10.11; found: C, 41.52; H, 2.98; N, 10.02. IR (KBr): *v*= 3427 (m), 1649 (w), 1625 (w), 1612 (s), 1583 (w), 1544 (m), 1508 (m), 1448 (s), 1404 (m), 1365 (m), 1336 (w), 1309 (w), 1230 (w), 1211 (m), 1184 (w), 1161 (m), 1132 (m), 1083 (s), 1047 (w), 1012 (m), 968 (s), 900 (m), 829 (w), 808 (m), 785 (m), 746 (m), 725 (m), 702 (w), 657 (m), 611 (m), 561 (s), 515 (m).

X-ray Crystallographic study. Single-crystal X-ray diffraction data for compound 1-3 were collected using a Bruker Apex II CCD diffractometer with Mo-Kα radiation (λ = 0.71073 Å). The structures of crystals were solved and refined using the SHELXTL package. Crystallographic parameters for all compounds are summarized in Table S1. Analysis of bond lengths and bond angles are included in Table S2-S4.

Proton Conductivity measurement. The grounded powder samples were compressed into pellets of 10 mm in diameter under a pressure of 15 MPa for 1 min. Impedance analysis of samples were determined using an IviumStat electrochemical workstation in the frequency range 1 - 1 MHz under an input voltage of 50 mV with a quasi-four-probe alternating current (AC) impedance method. The measurement conditions are controlled using a constant humidity and temperature incubator (BPHS-060A). The impedance results was extrapolated from the Nyquist plots using ZsimpWin software procedure by dint of an equivalent circuit simulation.

D_2O-exchanged experiment. For D_2O exchange, the grounded as-synthesized samples were pretreated for 24 h at 373 K. The dehydrated samples were compressed into pellets and were exposed to saturated aqueous salt solution of K_2SO_4 (~97% RH) to balance for 24 h at 298 K, of which K_2SO_4 was dissolved into D_2O solvent. Then the pellets were used to measure impedance data.

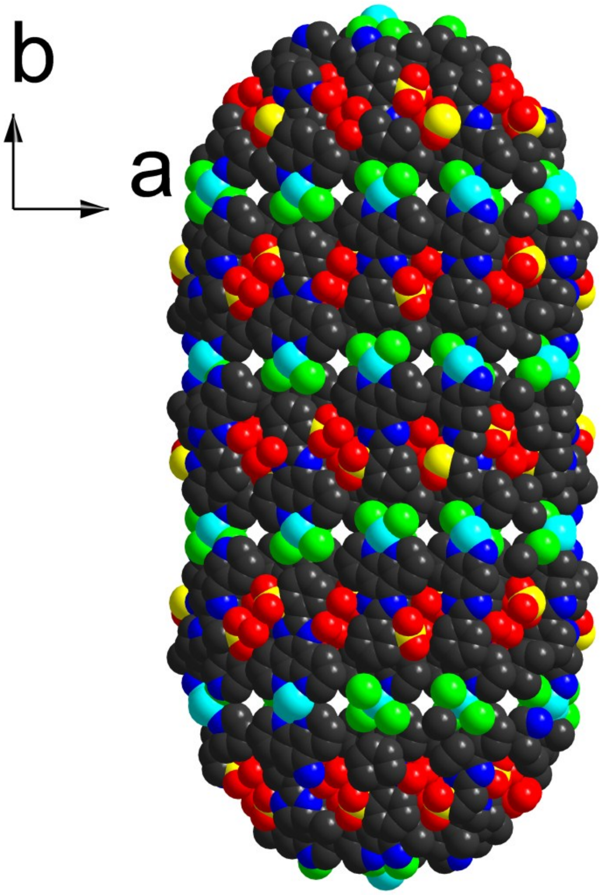

Figure S1. View of the packing arrangement of compound **2** along c axis on the space filling models.

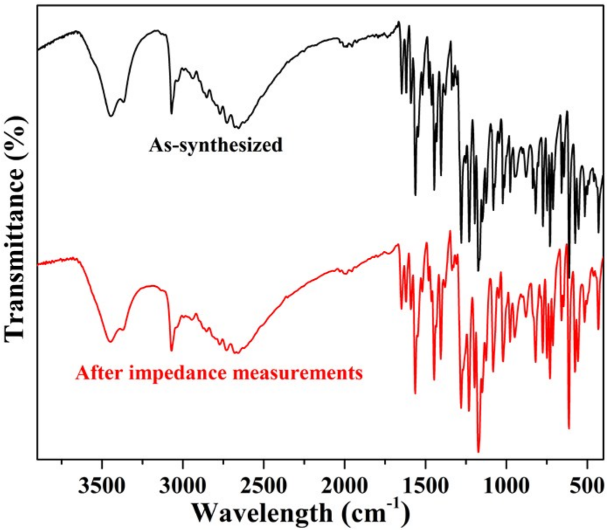

Figure S2. FT-IR spectra of compound **1** before and after impedance measurements.

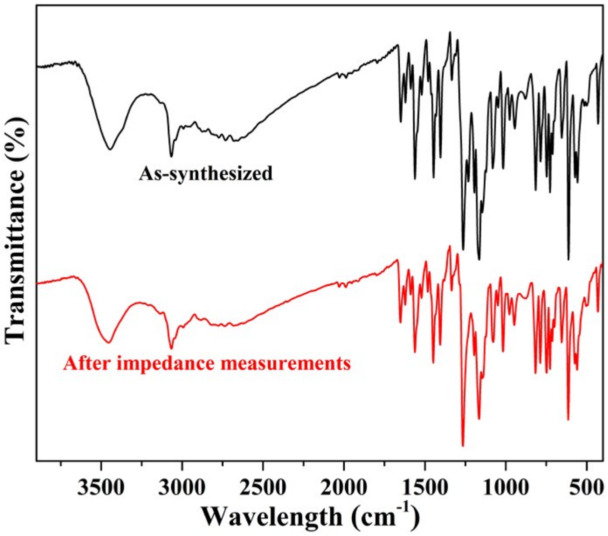

Figure S3. FT-IR spectra of compound **2** before and after impedance measurements.

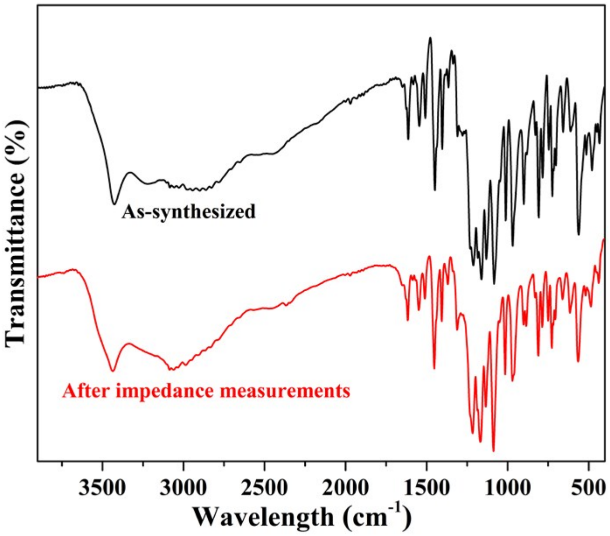

Figure S4. FT-IR spectra of compound **3** before and after impedance measurements.

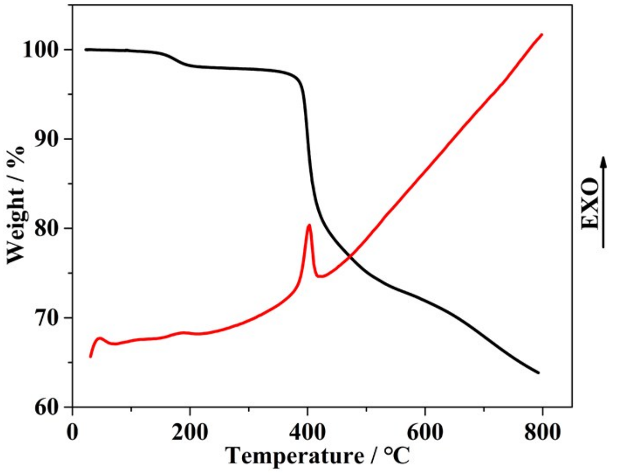

Fig S5. TGA and DSC curves of compound **1**.

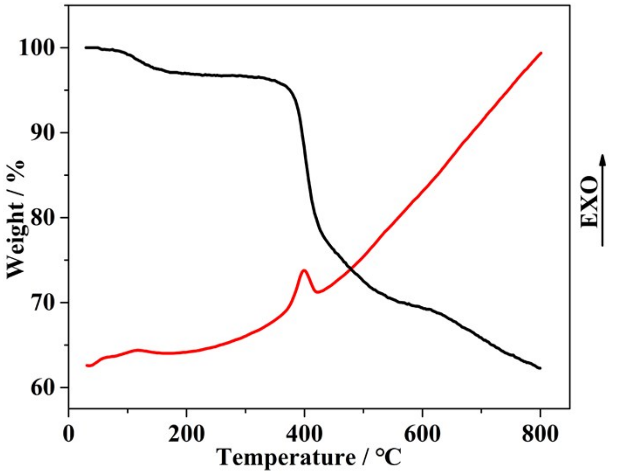

Fig S6. TGA and DSC curves of compound **2**.

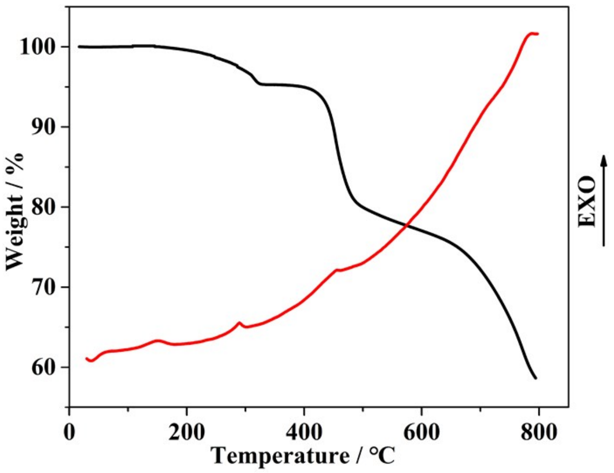

Fig S7. TGA and DSC curves of compound **3**.

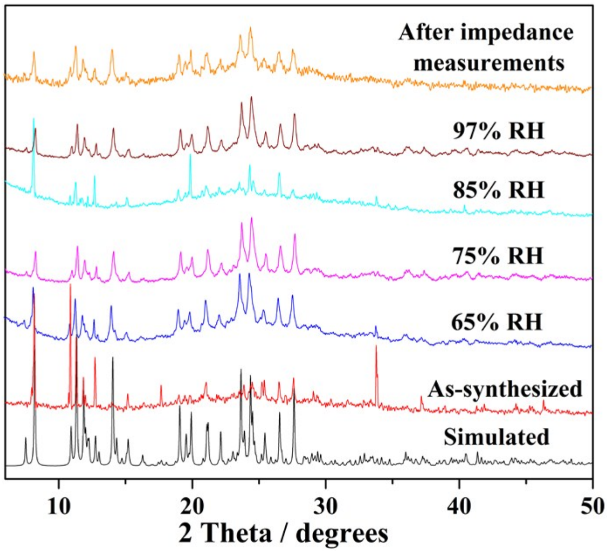

Fig S8. PXRD patterns of compound **1**; simulated pattern, as-synthesized pattern, variable-humidity PXRD patterns at 25 °C and 65% RH, 75% RH, 85% RH and 97% RH and after impedance measurements.

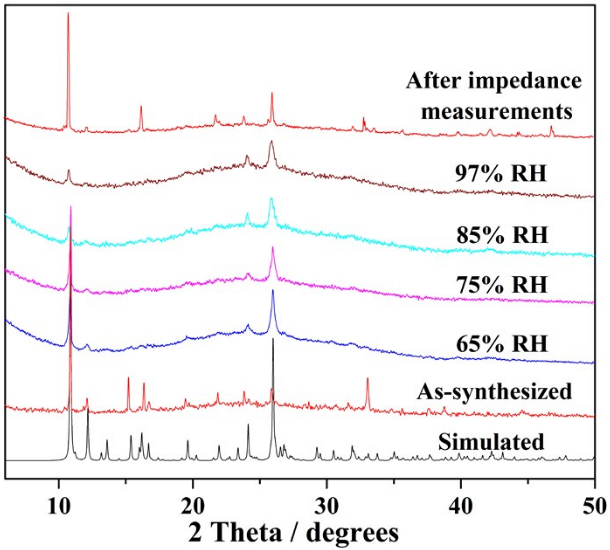

Fig S9. PXRD patterns of compound **2**; simulated pattern, as-synthesized pattern, variable-humidity PXRD patterns at 25 °C and 65% RH, 75% RH, 85% RH and 97% RH and after impedance measurements.

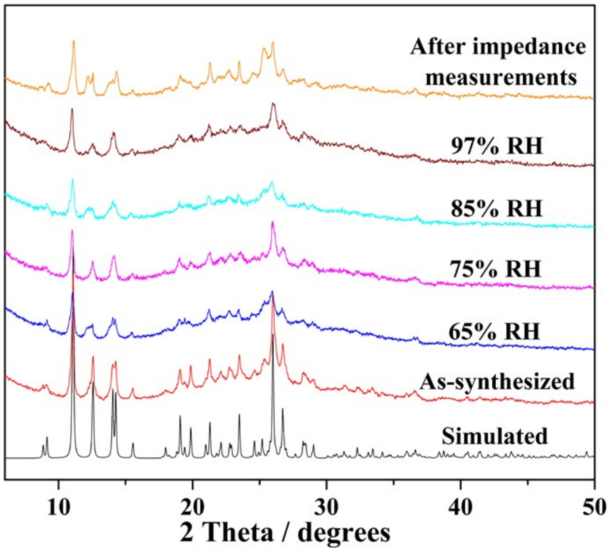

Fig S10. PXRD patterns of compound **3**; simulated pattern, as-synthesized pattern, variable-humidity PXRD patterns at 25 °C and 65% RH, 75% RH, 85% RH and 97% RH and after impedance measurements.

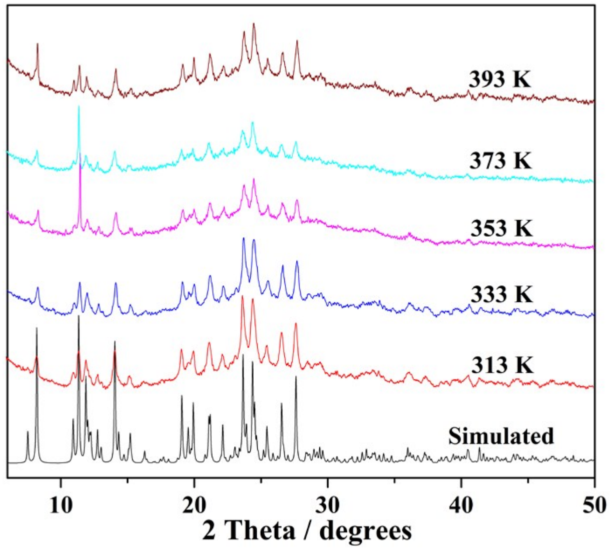

Fig S11. Simulated and variable-temperature PXRD patterns of compound **1**.

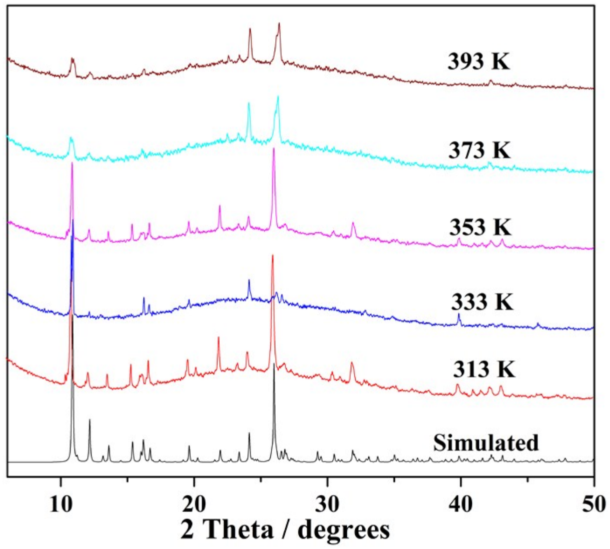

Fig S12. Simulated and variable-temperature PXRD patterns of compound **2**.

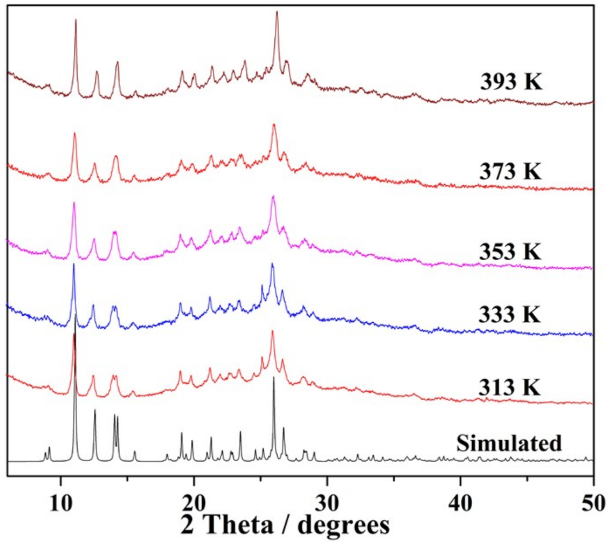

Fig S13. Simulated and variable-temperature PXRD patterns of compound **3**.

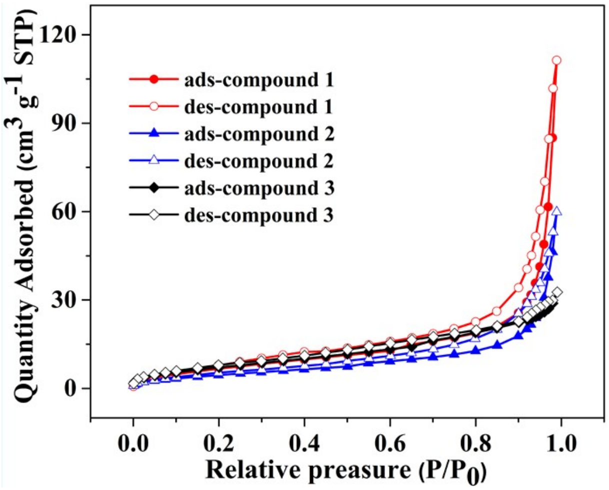

Fig S14. N_2 adsorption isotherms for three compounds at 77 K.

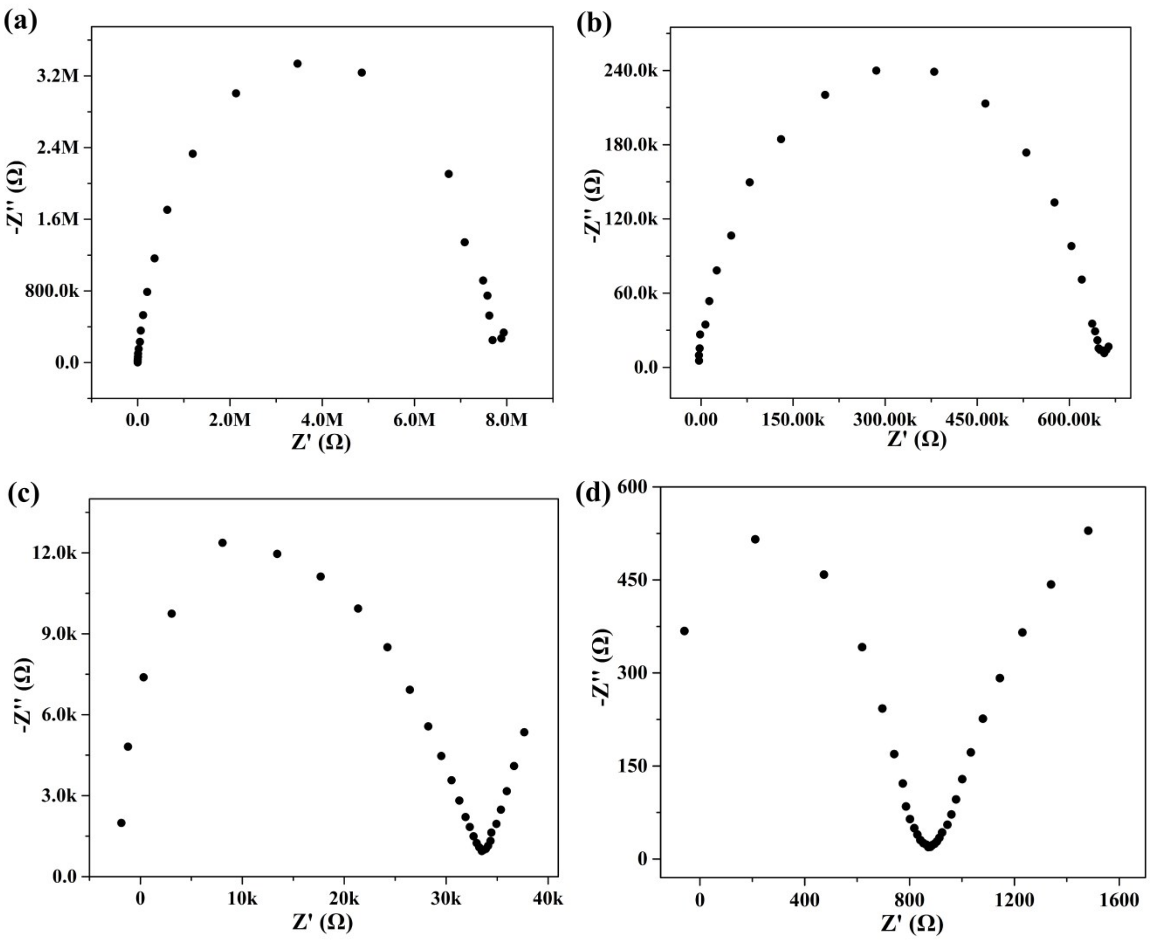

Fig S15. Nyquist plot of compound **1** at 25 °C and 65% RH (a), 75% RH (b), 85% RH (c) and 97% RH (d).

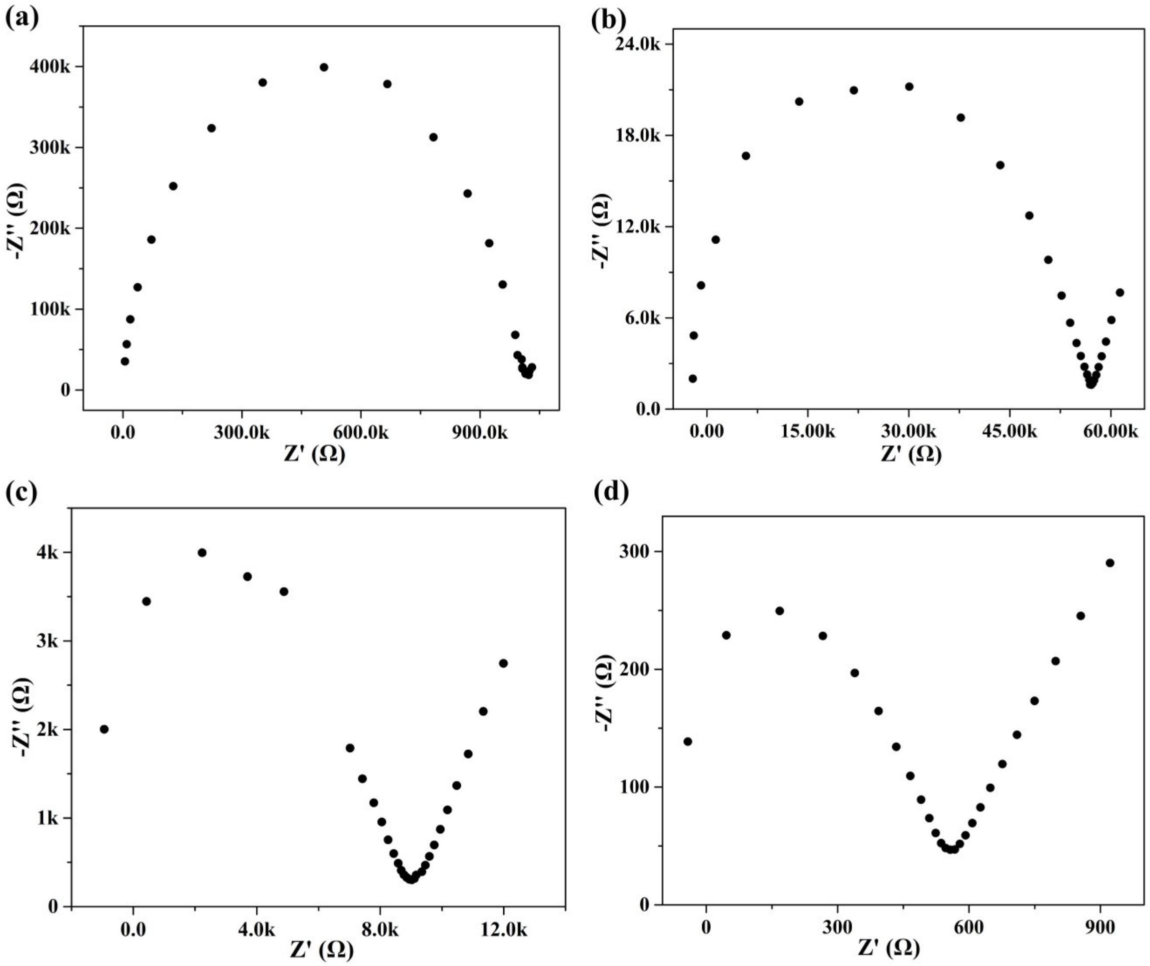

Fig S16. Nyquist plot of compound **2** at 25 °C and 65% RH (a), 75% RH (b), 85% RH (c) and 97% RH (d).

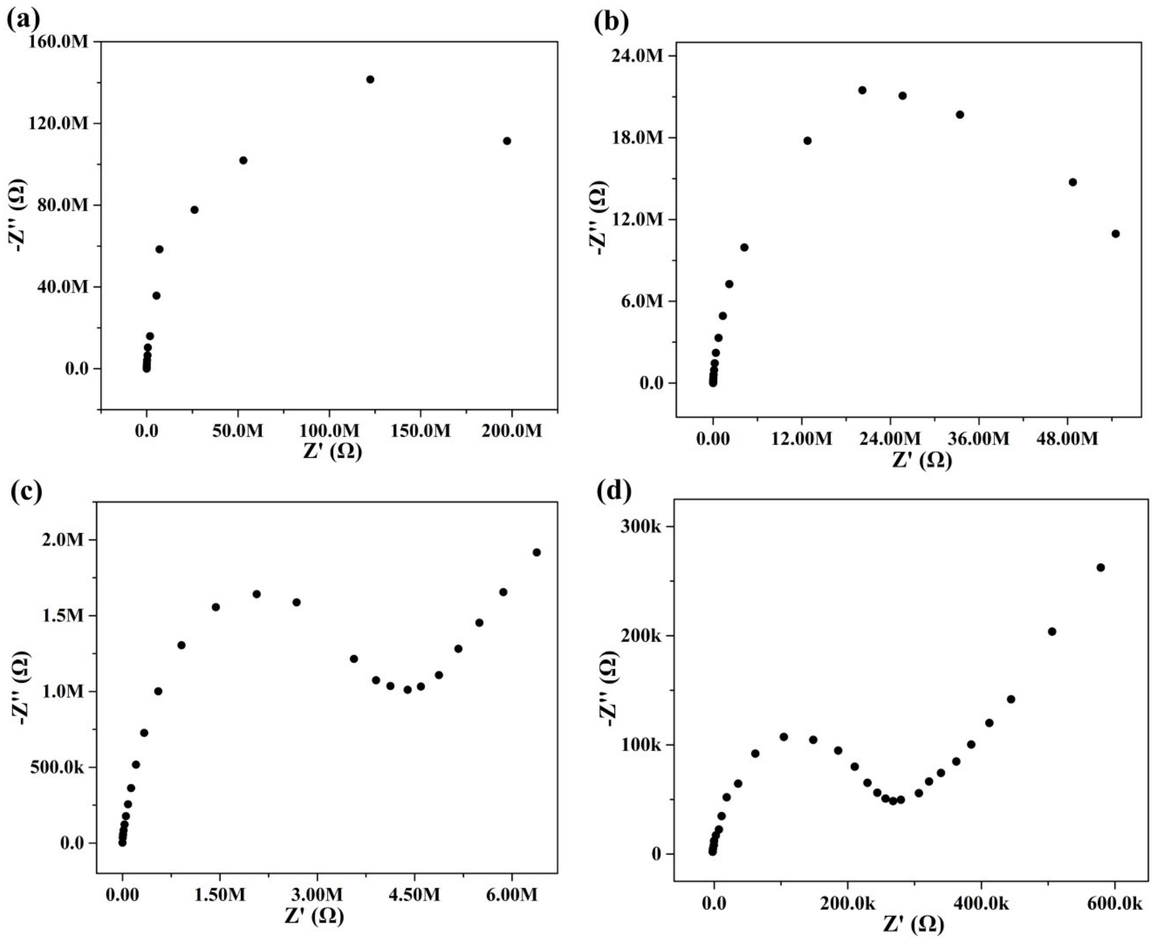

Fig S17. Nyquist plot of compound **3** at 25 °C and 65% RH (a), 75% RH (b), 85% RH (c) and 97% RH (d).

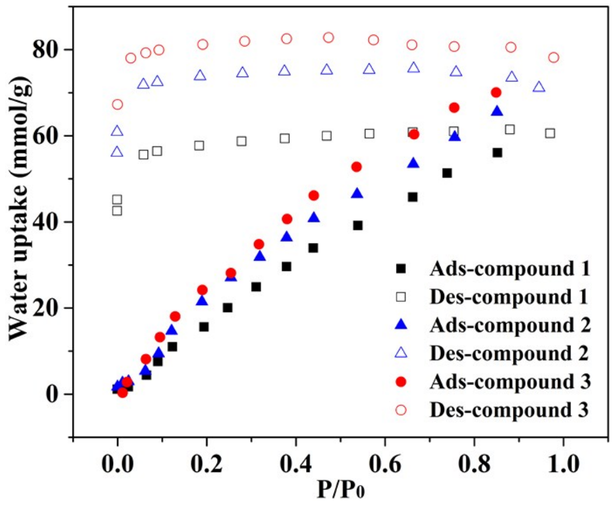

Fig S18. Water vapor adsorption isotherms of three compounds at 25°C.

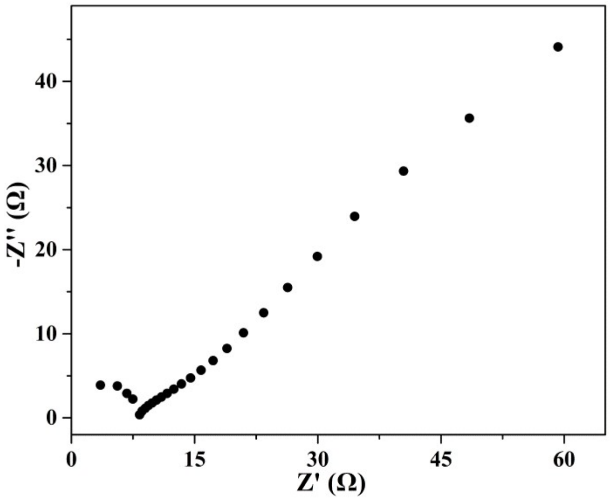

Fig S19. Nyquist plot of compound **1** at 95 °C under 97% RH.

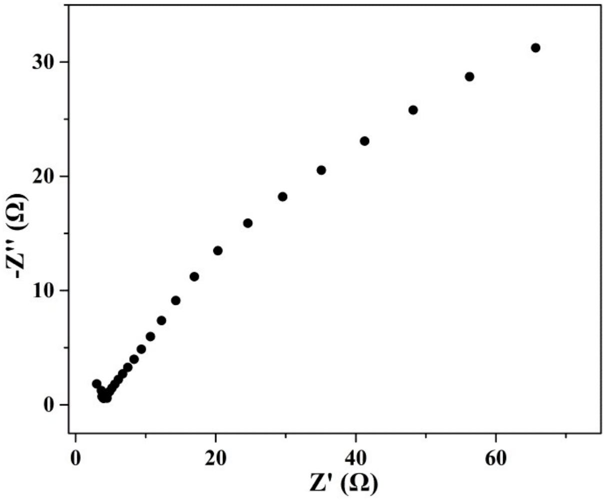

Fig S20. Nyquist plot of compound **2** at 95 °C under 97% RH.

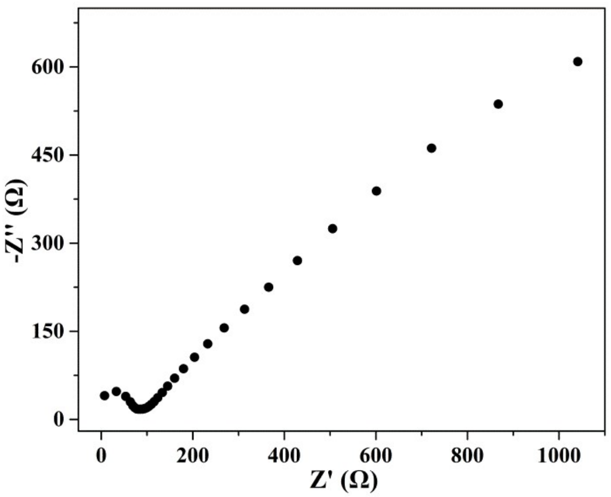

Fig S21. Nyquist plot of compound **3** at 95 °C under 97% RH.

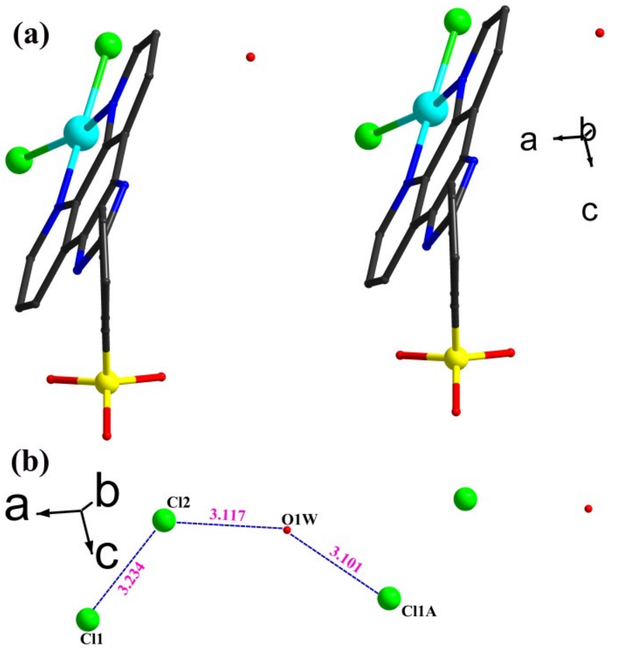

Fig S22. (a) Overview of representation of hydrogen-bond network of compound **1**. (b) Segment of representation of hydrogen-bond network of compound **1**.

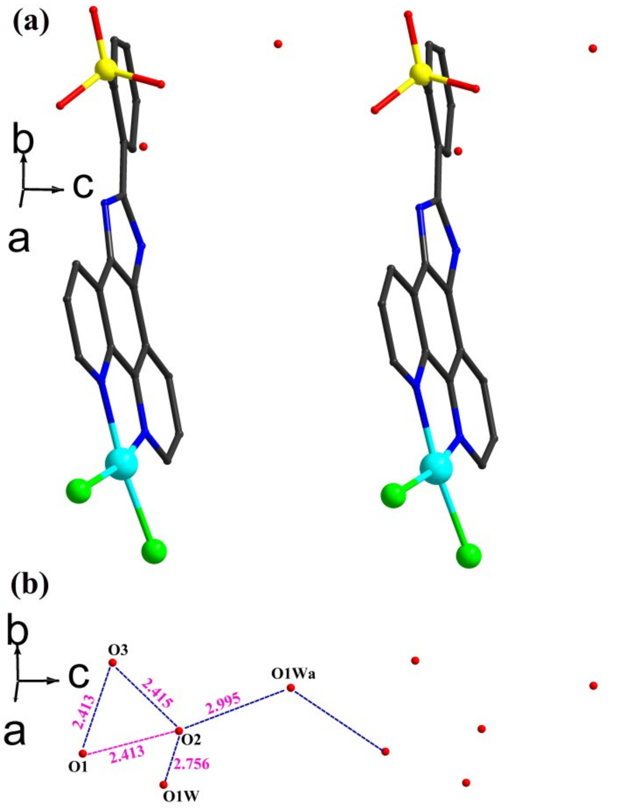

Fig S23. (a) Overview of representation of hydrogen-bond network of compound **2**. (b) Segment of representation of hydrogen-bond network of compound **2**.

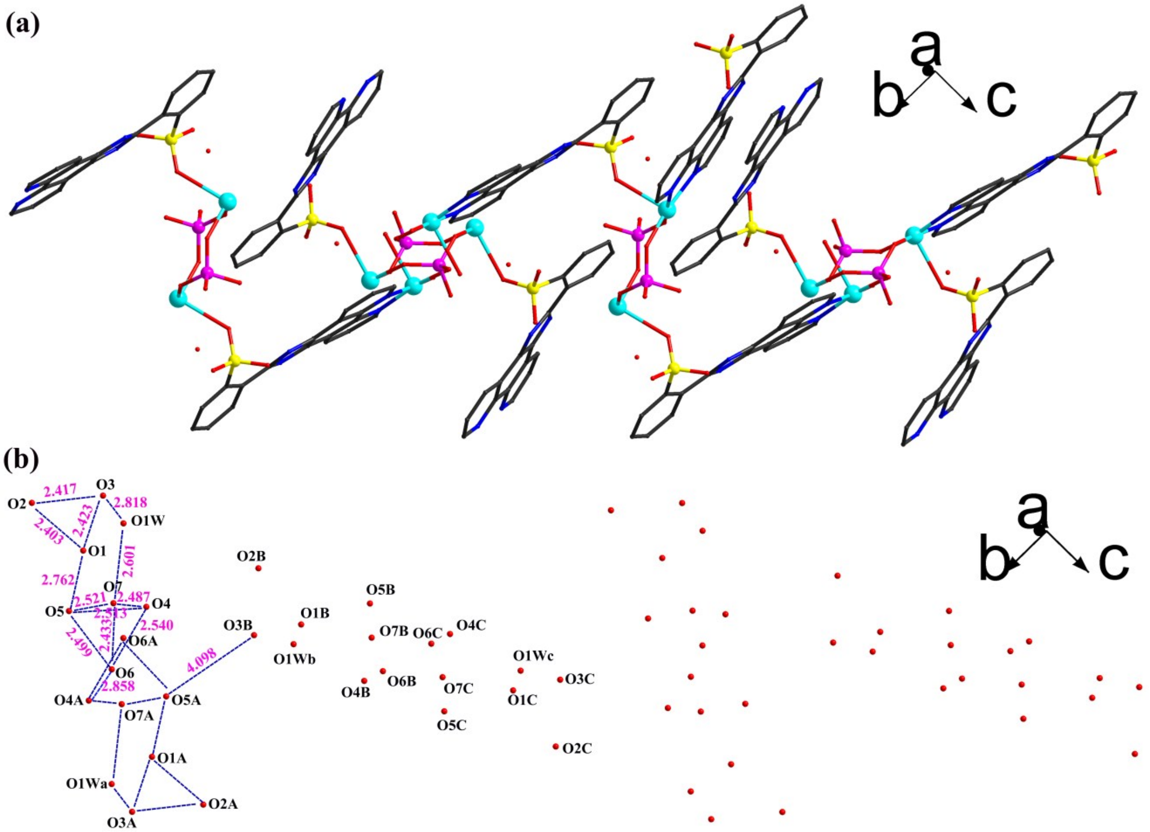

Fig S24. (a) Overview of representation of hydrogen-bond network of compound **3**. (b) Segment of representation of hydrogen-bond network of compound **3**.

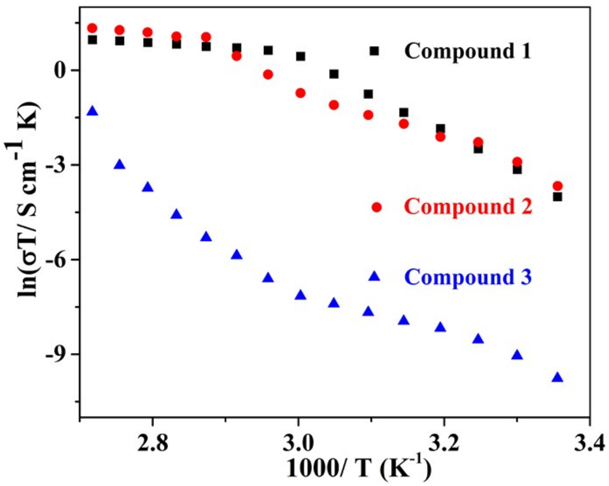

Fig S25. Arrhenius plots of the proton conductivity of all compounds from 25 to 95 °C at 97% RH.

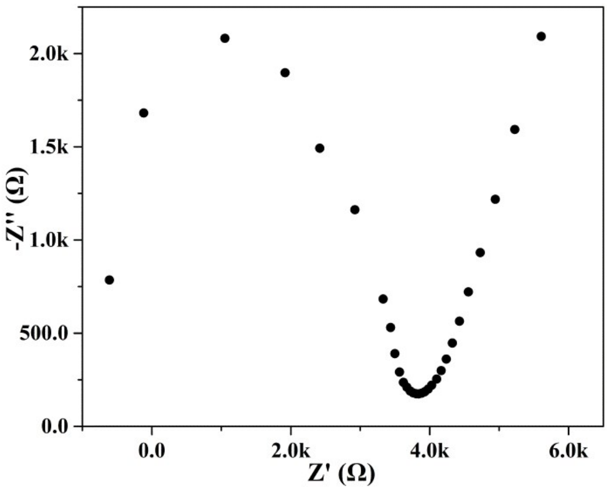

Fig S26. Nyquist plot of compound **1** in presence of D_2O at 25 °C under 97% RH.

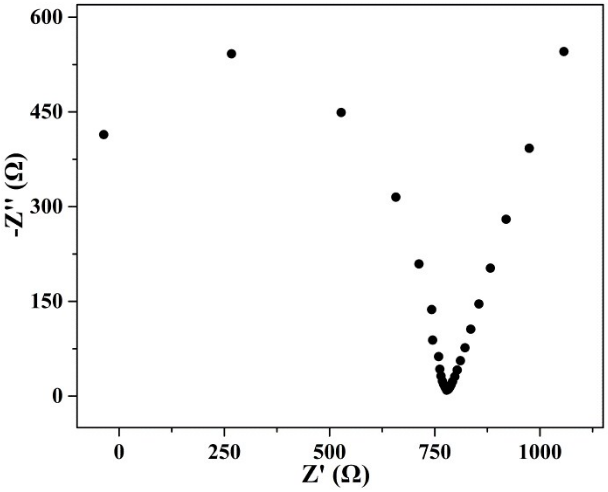

Fig S27. Nyquist plot of compound **2** in presence of D_2O at 25 °C under 97% RH.

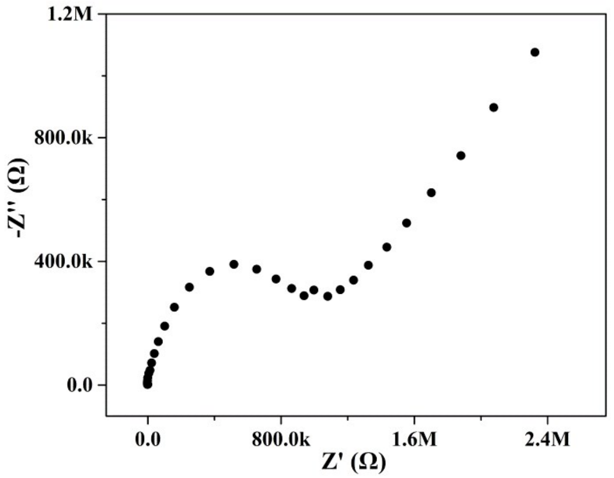

Fig S28. Nyquist plot of compound **3** in presence of D_2O at 25 °C under 97% RH.

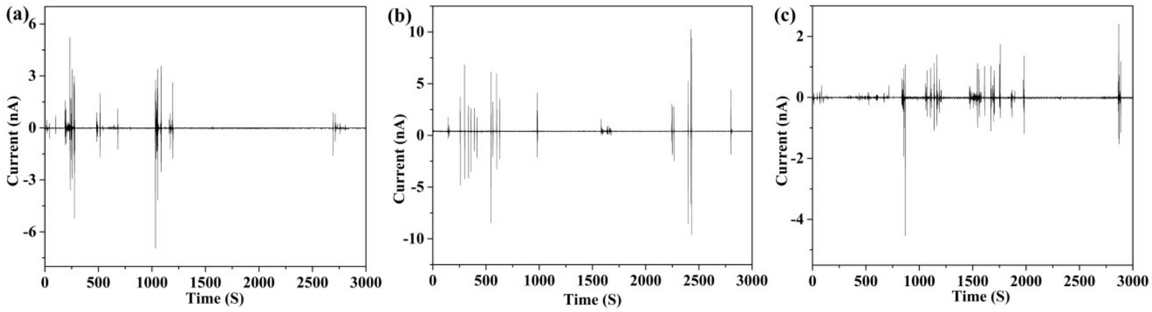

Fig S29. Time-current relationship in Hebb-Wagner polarization method for compound **1** (a), **2** (b), **3** (c).

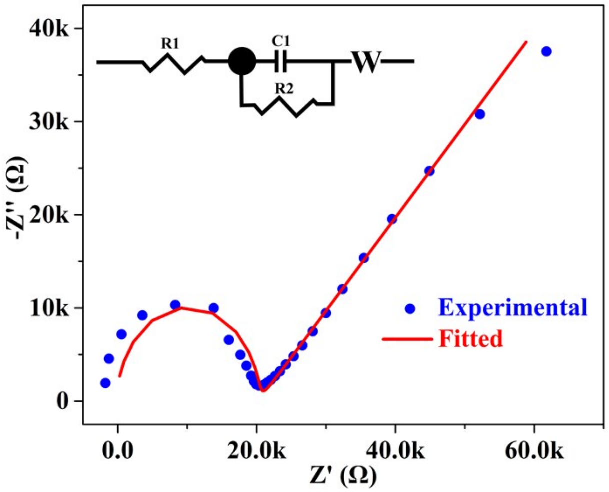

Fig S30. Fitting for the Nyquist plot at 60 °C and 97%RH conditions of compound **3**, with circuit model used for the data fitting shown as an inset.

Table S1. Crystal data and structure refinements for compound **1**、compound **2** and compound **3**.

Compound reference	**1**	**2**	**3**
Chemical formula	$C_{38}H_{26}N_8O_7Cu_2S_2Cl_4$	$C_{19}H_{14}N_4O_4CuSCl_2$	$C_{19}H_{15}N_4O_8CuSP$
Formula Mass	1039.67	528.84	553.92
Crystal system	triclinic	monoclinic	monoclinic
a/(Å)	7.629(5)	8.124(5)	10.350(5)
b/(Å)	15.946(5)	32.652(5)	14.076(5)
c/(Å)	16.469(5)	7.379(5)	14.963(5)
α/°	92.875(5)	90.000(5)	90.000(5)
β/°	99.764(5)	93.140(5)	109.222(5)
γ/°	101.239(5)	90.000(5)	90.000(5)
Unit cell volume/(Å)$_3$	1929.4(15)	1954.5(18)	2058.4(14)
Temperature/K	293(2)	293(2)	293(2)
Space group	P -1	P 21/c	P 21/n
No. of formula units per unit cell, Z	2	4	4
No. of reflections measured	7084	4856	5045
No. of independent reflections	4458	3330	3342
R_{int}	0.0459	0.0642	0.0538
Final R_1 values (I> $2\sigma(I)$)^a	0.0578	0.0808	0.0489
Final $wR(F_2)$ values (I> $2\sigma(I)$)^b	0.1386	0.1745	0.1266
Final R_1 values (all data)	0.1092	0.1184	0.0869
Final $wR(F_2)$ values (all data)	0.1847	0.1903	0.1456
Goodness of fit on F_2	1.052	1.119	1.024

$^aR_1=\Sigma||Fo|-|Fc||/\Sigma|Fo|$. $^bwR_2= |\Sigma w(|F_o|^2-|F_c|^2)|/\Sigma|w(F_o^2)^2|^{1/2}$

Table S2. Selected bond lengths [Å] for compound **1**.

N(1)-Cu(1)	2.033(6)	Cu(1)-Cl(1)	2.251(2)
N(2)-Cu(1)	2.027(6)	Cu(1)-Cl(2)	2.257(2)
N(5)-Cu(2)	2.052(6)	Cu(2)-Cl(4)	2.221(2)
N(6)-Cu(2)	2.034(6)	Cu(2)-Cl(3)	2.248(2)
O(4)-Cu(1)#1	2.275(5)	Cl(1)-Cu(1)-O(4)#2	92.00(14)
N(2)-Cu(1)-O(4)#2	104.0(2)	Cl(2)-Cu(1)-O(4)#2	93.51(14)
N(1)-Cu(1)-O(4)#2	89.1(2)		

Table S3. Selected bond lengths [Å] for compound **2**.

N(1)-Cu(1)	2.035(5)	N(2)-Cu(1)-N(1)	81.28(19)
N(2)-Cu(1)	2.020(5)	N(2)-Cu(1)-Cl(2)	172.63(16)
Cl(1)-Cu(1)	2.2480(19)	N(1)-Cu(1)-Cl(2)	93.07(14)
Cl(2)-Cu(1)	2.2435(18)	N(2)-Cu(1)-Cl(1)	92.46(15)
		N(1)-Cu(1)-Cl(1)	168.75(16)
		Cl(2)-Cu(1)-Cl(1)	93.86(7)

Table S4. Selected bond lengths [Å] for compound **3**.

N(1)-Cu(1)	2.006(3)	O(4)-Cu(1)-O(6)#1	96.24(12)
N(2)-Cu(1)	1.989(3)	O(4)-Cu(1)-N(2)	172.68(12)
O(4)-Cu(1)	1.917(3)	O(6)#1-Cu(1)-N(2)	90.79(12)
O(6)-Cu(1)#1	1.921(3)	O(4)-Cu(1)-N(1)	91.33(12)
		O(6)#1-Cu(1)-N(1)	168.77(13)

Table S5. Comparison of proton conductivity of compounds with sulfonate groups proton conductors.

Compounds	T (°C)	RH (%)	Proton conductivity (S cm^{-1})	Reference
UiO-66$(SO_3H)_2$	80	90	8.4×10^{-2}	*Angew. Chem. Int. Ed.*, 2015, **54**, 5142-5146.
TfOH@MIL-101	60	15	8×10^{-2}	*ACS Appl. Mater.Interfaces.*,2014, **6**, 5161- 5167.
H_2SO_4@ MIL-101	80	20	6×10^{-2}	*J. Am. Chem. Soc.*, 2012, **134**, 15640-15643.
$(Me_2NH_2)_3(SO_4)]_2[M_2(ox)_3]$	25	98	4.2×10^{-2}	*Angew. Chem. Int. Ed.*, 2014, **53**, 2638-2642.
HOF-GS-11	30	95	1.8×10^{-2}	*Angew. Chem. Int. Ed.*, 2016, 55, 10667-10671.
$CuH(Hsfpip)Cl(H_2O)$	95	97	1.50×10^{-2}	*J. Mater. Chem. A.*, 2017, **5**, 1085-1093.
$Cu(H_2spip)Cl_2{\cdot}H_2O$	95	97	1.09×10^{-2}	*This work.*
HOF-GS-10	30	95	0.75×10^{-2}	*Angew. Chem. Int. Ed.*, 2016, 55, 10667-10671.
$Cu_2H_2(Hspip)_2Cl_4{\cdot}H_2O$	95	97	6.47×10^{-3}	*This work.*
$Zr_6O_4(OH)_8L_{4.2}{\cdot}xH_2O$	65	95	5.62×10^{-3}	*J. Am. Chem. Soc.*, 2015, **137**, 11498-11506.
$[Cu(H_2L)(DMF)_4]_n$	95	95	3.46×10^{-3}	*Dalton Trans.*, 2015, **44**, 948-954.
H_3PO_4@MIL-101	150	0.13	3×10^{-3}	*J. Am. Chem. Soc.*, 2012, **134**, 15640-15643.
$CuH_2(Hsfpip)_2(H_2O)$	95	97	2.58×10^{-3}	*J. Mater. Chem. A.*, 2017, **5**, 1085-1093.
Cu-DSOA	85	98	1.9×10^{-3}	*Chem. Commun.*, 2013, **49**, 10590-10592.
$Cu(Hsfpip)(H_2O)_2{\cdot}H_2O$	95	97	1.43×10^{-3}	*J. Mater. Chem. A.*, 2017, **5**, 1085-1093.
$CB[6]{\cdot}1.2H_2SO_4{\cdot}6.4H_2O$	25	98	1.3×10^{-3}	*Angew. Chem. Int. Ed.*, 2011, **34**, 7870-7873.
$Cu_4(L)_2(OH)_2(DMF)_2$	95	95	7.4×10^{-4}	*Chem. Commun.*, 2015, **51**, 8150-8152.
$CuH(Hspip)(HPO_4){\cdot}H_2O$	95	97	6.90×10^{-4}	*This work.*
$Cu_2(H_2spip)_2(HPO_4)O{\cdot}1.5H_2O$	95	97	5.11×10^{-4}	*This work.*
$[Zn(5\text{-}sipH)(bpy)]{\cdot}DMF{\cdot}2H_2O$	25	60	3.9×10^{-4}	*Chem. Commun.*, 2014, **50**, 1144-1146.
Tb-DSOA	100	98	1.66×10^{-4}	*J. Mater. Chem. A.*, 2015, **3**, 641-647.
$[Zn_3(5\text{-}sip)_2(5\text{-}sipH)(bpy)] \cdot (DMF) {\cdot}2(DMA)$	25	60	8.7×10^{-5}	*Chem. Commun.*, 2014, **50**, 1144-1146.
$[\{In_2(\mu\text{-}OH)_2(SO_4)_4\}{\cdot}\{(LH)_4\}{\cdot}nH_2O]n$	30	98	4.4×10^{-5}	*Inorg. Chem.*, 2015, **54**, 5366-5371.
Sr-SBBA	25	98	4.4×10^{-5}	*Chem. Commun.*, 2012, **48**, 4998-5000.
$\{[Cu(pyz)(5\text{-}Hsip)(H_2O)_2].(H_2O)_2\}_n$	65	95	3.5×10^{-5}	*Inorg. Chem.*, 2017, **56**, 1581-1590.
TsOH@MIL-101	50	100	3×10^{-5}	*ACS Appl. Mater.Interfaces.*, 2014, **6**, 5161-5167.
$[CaL_{0.5}(DMF)_{2.5}]_n$	95	95	1.27×10^{-5}	*Dalton Trans.*, 2015, **44**, 948-954.
Ca-SBBA	25	98	8.58×10^{-6}	*Chem. Commun.*, 2012, **48**, 4998-5000.
$\{[Cu(bpy)(5\text{-}Hsip)(H_2O)]{\cdot}(H_2O)_2\}_n$	65	95	5.8×10^{-6}	*Inorg. Chem.*, 2017, **56**, 1581-1590.
$\{[Zn(bpeH)(5\text{-}sip)(H_2O)]{\cdot}(H_2O)\}_n$	65	95	2.5×10^{-6}	*Inorg. Chem.*, 2017, **56**, 1581-1590.
$\{[Cu(bpy)_2(5\text{-}H_2sip)_2]{\cdot}(H_2O)_6\}_n$	65	95	1.4×10^{-6}	*Inorg. Chem.*, 2017, **56**, 1581-1590.
$[CdL_{0.5}(DMF)_2]_n$	95	95	2.49×10^{-7}	*Dalton Trans.*, 2015, **44**, 948-954.
$\{[Cu(bpee)_{0.5}(5\text{-}sip)(H_2O)_2]{\cdot}(H_2O)_4(bpeeH_2)_{0.5}\}_n$	65	95	9.9×10^{-8}	*Inorg. Chem.*, 2017, **56**, 1581-1590.
$[Zn(H_2O)(5\text{-}sipH)(bpe)_{0.5}] {\cdot}DMF$	25	60	3.4×10^{-8}	*Chem. Commun.*, 2014, **50**, 1144-1146.

Table S6. Comparison of proton conductivity among some reported MOFs.

Compounds	T (°C)	RH (%)	Proton conductivity (S cm^{-1})	Reference
UiO-66$(SO_3H)_2$	80	90	8.4×10^{-2}	*Angew. Chem. Int. Ed.*, 2015, **54**, 5142-5146.
Fe-CAT-5	25	98	5×10^{-2}	*J. Am. Chem. Soc.* 2015., **137**, 15394-15397.
$(Me_2NH_2)_3(SO_4)]_2[M_2(ox)_3]$	25	98	4.2×10^{-2}	*Angew. Chem. Int. Ed.*, 2014, **53**, 2638-2642.
PCMOF-10	60	95	3.55×10^{-2}	*J. Am.Chem. Soc.*, 2015, **137**, 7640-7643.
H+@Ni_2(dobdc)$(H_2O)_2$ (pH = 1.8)	80	98	2.2×10^{-2}	*Angew.Chem. Int. Ed.*, 2014, **53**, 8383-8387.
PCMOF2$^{1}/_{2}$	85	90	2.1×10^{-2}	*J. Am. Chem. Soc.*, 2013, **135**, 963-966.
CuH(Hsfpip)Cl(H_2O)	95	97	1.50×10^{-2}	*J. Mater. Chem. A.*, 2017, **5**, 1085-1093.
Im–Fe–MOF	60	98	1.21×10^{-2}	10.1021/jacs.7b01559
Cu$(H_2$spip$)Cl_2 \cdot H_2O$	95	97	1.09×10^{-2}	*This work.*
$(NH_4)_2(H_2$adp$)[Zn_2(ox)_3] \cdot 3H_2O$	25	98	8×10^{-3}	*J. Am. Chem. Soc.*, 2014, **136**, 7701-7707.
Cu_2H_2(Hspip)$_2Cl_4 \cdot H_2O$	95	97	6.47×10^{-3}	*This work.*
PCMOF-5	62	98	4×10^{-3}	*J. Am. Chem. Soc.*, 2013, **135**, 1193-1196.
(Me_2NH_2)[Eu(L)]	100	98	3.76×10^{-3}	*J. Am. Chem. Soc.*, 2017, **139**, 3505-3512.
$[Me_2NH_2][Eu(ox)_2(H_2O)] \cdot 3H_2O$	55	95	2.73×10^{-3}	*J. Mater. Chem. A.*, 2016, **4**, 16484-16489.
CuH_2(Hsfpip)$_2(H_2O)$	95	97	2.58×10^{-3}	*J. Mater. Chem. A.*, 2017, **5**, 1085-1093.
Cu(Hsfpip)$(H_2O)_2 \cdot H_2O$	95	97	1.43×10^{-3}	*J. Mater. Chem. A.*, 2017, **5**, 1085-1093.
Fe(ox) $\cdot 2H_2O$	25	98	1.3×10^{-3}	*J. Am. Chem. Soc.*, 2009, **131**, 3144-3145.
CoCa$\cdot nH_2O$	25	95	1×10^{-3}	*Chem. Mater.*, 2015, **27**, 8116-8125.
{[Ca(D-Hpmpc)$(H_2O)_2$] $\cdot 2HO_{0.5}\}_n$	60	97	8.9×10^{-4}	*Chem. Sci.*, 2013, **4**, 983-992.
$Ca^{II}Cu^{II}{}_6$[(*S,S*)-alamox]$_3(OH)_2(H_2O)$	80	95	8.6×10^{-4}	*Chem. Mater.*, 2016, **28**, 4608-4615.
CuH(Hspip)$(HPO_4) \cdot H_2O$	95	97	6.90×10^{-4}	*This work.*
MFM-500(Ni)	25	98	4.5×10^{-4}	*J. Am. Chem. Soc.*, 2016, **138**, 6352-6355.
In-IA-2D-2	27	98	4.2×10^{-4}	*Chem. Commun.*, 2013, **49**, 6197-6199.
$K_2(H_2$adp$)[Zn_2(ox)_3] \cdot 3H_2O$	25	98	1.2×10^{-4}	*J. Am. Chem. Soc.*, 2014, **136**, 13166-13169.
{NH(prol)$_3$}[MCr(ox)$_3$]	25	75	1.0×10^{-4}	*J. Am. Chem. Soc.*, 2009, **131**, 13516-13522.
$[NMe_3(CH_2CO_2H)][FeCr(ox)_3] \cdot nH_2O$	25	65	8.0×10^{-5}	*J. Am. Chem. Soc.*, 2012, **134**, 5472-5475.
In-5TIA	28	98	5.35×10^{-5}	*Chem. Commun.*, 2012, **48**, 5464-5466.
$(Me_2NH_2)_2[Li_2Zr(C_2O_4)_4]$	17	67	3.9×10^{-5}	*J. Am.Chem. Soc.*, 2015, **137**, 6428-6431.

Reference

(1) Xu, B.; Chen, Q.; Hu, H. M.; An, R.; Wang, X. F.; Xue, G. L. *Cryst. Growth Des*. **2015**, *15*, 2318-2329.

(2) Zhou, E. L.; Qin, C.; Wang, X. L.; Shao, K. Z.; Su, Z. M. *Chem. Eur. J.* **2015**, *21*, 13058-13064.